

SUBMILLISECOND CHROMIUM ION BEAMS WITH HIGH-PULSE POWER DENSITY

A. V. Gurulev and A. I. Ryabchikov

UDC 533.93:537.525

The paper focuses on the formation of high-intensity submillisecond chromium ion beams with a high power density. The ion-induced electron emission at the energy reaching 70 keV affects the neutralization of space charge and determination accuracy of the ion beam parameters. It is shown that at high ion energies, the virtual anode effect does not appear, and the formation of ion beams of a high pulse duration occurs. It is found that at 170 A discharge current, the maximum current density averaged over 16 pulses, reaches 2.8 A/cm². The maximum power density in the ion beam at 35 kV accelerating voltage approaches to 100 kW/cm². Instability of the ion-induced electron emission from the vacuum arc plasma improves the power density of pulses by more than 2 times.

Keywords: chromium ion, submillisecond pulses, repetitively pulsed mode, high-power density.

INTRODUCTION

Ion implantation possesses unique properties and monitors changes in the elemental and phase composition and surface microstructure of the material, in particular semiconductors [1, 2]. The use of conventional ion implantation for the property modification of metals and alloys, is restricted by a small projective range of ions with a duration not exceeding several tens of nanometers [3–10]. A number of works describe a breakthrough concerning an increase in the ion-doped layer depth when implanting nitrogen ions into different types of steel. Researchers demonstrate the possibility of increasing the ion-doped layer up to several tens of micrometers when implanting low-energy nitrogen ions not over 1.5 keV due to the beam current density increased to 2 mA/cm². This method is called high-current, low-energy ion implantation [11, 12]. At such current density, blocking of the nitrogen diffusion in various steel types by the surface oxidation, is eliminated. The generation of low-energy metal and gas ion beams with a high current density of 1 A/cm², provide a strong push to the ion implantation in metals and alloys [13]. In our recent research [14] we show the fundamental possibility of the multiple amplification of radiation-induced diffusion with the achievement of high growth rates deep into the ion-doped layers. The high-intensity implantation of low-energy ions demonstrates promising applications of nitrogen ion beams and other chemical elements with a small atomic radius in the targeted formation of the elemental composition and microstructure in the surface layers of various metals and alloys with a thickness of several tens and even hundreds of micrometers. However, large-scale applications of the high-intensity implantation of a wide range of low-energy ions in metals and alloys require high temperatures, which significantly increase the grain size of crystal structures and can degrade the performance properties of processed materials. It should be noted that the high-intensity implantation of low-energy ions is accompanied by the temperature growth throughout the volume of the processed product.

A new approach to the high-intensity implantation is proposed in [15]. It is based on synergy of the high-intensity implantation of medium energy ions and the impact of the ion beam energy on the surface, which involve repetitively-pulsed heating of the surface layer up to temperatures ensuring an enhanced radiation-induced diffusion.

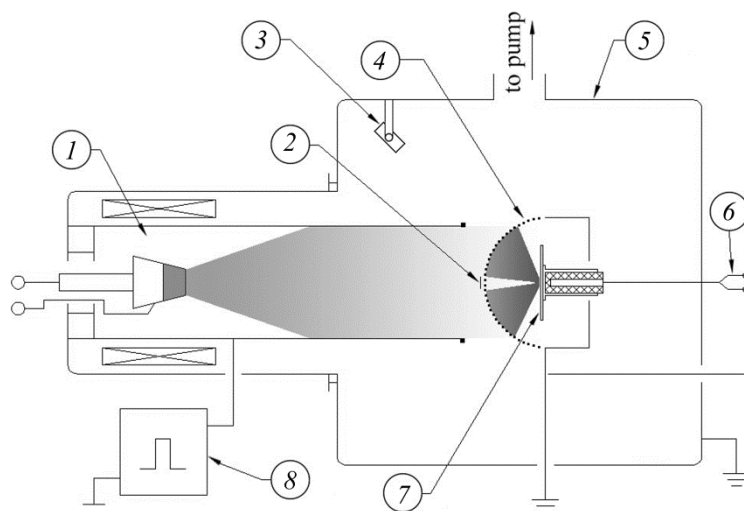


Fig. 1. Schematic of the ion-beam and ion-plasma system: 1 – vacuum-arc plasma generator, 2 – cut-off electrode, 3 – pulse pyrometer, 4 – grid electrode, 5 – vacuum chamber, 6 – thermocouple, 7 – continuous collector, 8 – repetitively-pulsed high-voltage generator.

The implementation of this method requires submillisecond repetitively-pulsed ion beams with a power density ranging between several units and several hundred kilowatts per square centimeter.

This work is devoted to the formation of high-intensity submillisecond chromium ion beams with a high pulse power density.

MATERIALS AND METHODS

Figure 1 presents a schematic view of the ion-beam and ion-plasma system for processing of materials [16]. A chromium plasma flow generates in the vacuum-arc generator of the ion-plasma source “Raduga-5”. The ion extraction from the free plasma boundary and their ballistic focusing are performed using the grid electrode with the radius of 130 mm, $1.2 \times 1.1 \text{ mm}^2$ cell, and 60% transparency. During the ballistic focusing, the beam drift space is restricted by a cylinder with the radius 100 mm and 175 mm length.

The experiments were conducted at a continuous discharge current of 130 to 170 A. Two repetitively-pulsed bias potential generators of positive polarity were used in experiments. The high-frequency generator with a frequency of 1 kHz and pulse duration of 100 μs generated positive polarity potentials ranging from 100 to 1800 V. The high-voltage pulse generator provided bias potentials of 5 to 35 kV and 450 μs duration. The disk electrode preventing a direct microparticle flow from the cathode surface to the beam focusing region, was placed at the focusing electrode center. The pulse frequency of accelerating voltage did not exceed 2 pps to avoid the collector overheat under at the ballistic beam focusing. Due to instability of the ion saturation current from the vacuum-arc plasma, current records were averaged on an LeCroy oscilloscope in order to improve the measurement accuracy. In the case of the high-frequency generator, averaging was carried out over 1024 pulses. At the high bias potential, averaging was carried out over 16 pulses to avoid the target overheat. The average temperature of the irradiated target was measured by a chromel-alumel thermocouple. A high-speed KLEIBER KGA 740-LO infrared pyrometer was used to measure the temperature changes on the irradiated target surface.

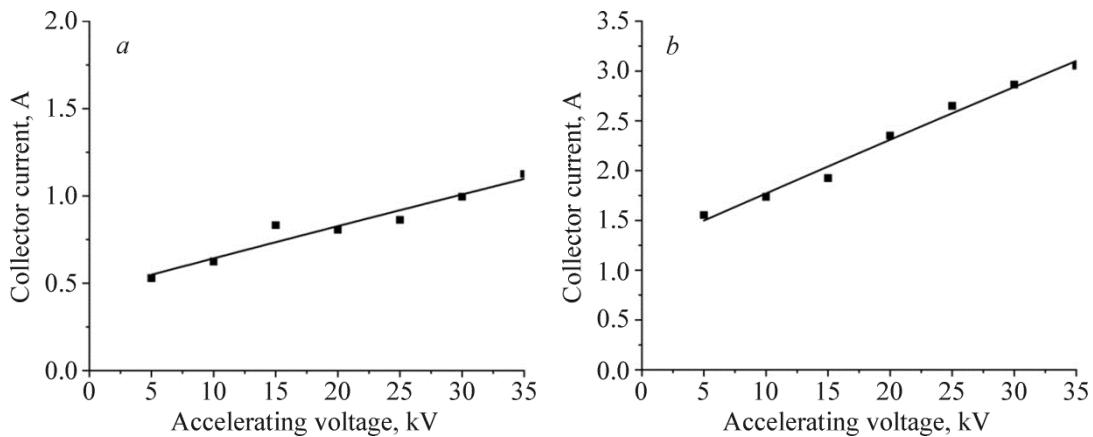


Fig. 2. Dependences between collector current and accelerating voltage during ballistic beam focusing at different discharge currents: *a* – 130 A, *b* – 170 A.

RESULTS AND DISCUSSION

The formation of high-intensity beams of chromium ions with the high power density at the accelerating voltage of several tens of kilovolts is characterized by remarkable properties. First of all, no virtual anode effect is observed at high values of the accelerating voltage, which restricts the pulse duration of the ion beam. The 450 μs ion beam consistently moves in the ballistic focusing conditions, without instabilities accompanied by the pulse duration shortening to 13–15 μs , typical for low-energy ion beams [13]. Second, a significant dependence of the current amplitude measured by the collector in the focal region of the ballistic beam focusing system, on the ion energy. Figure 2*a* shows the dependence between the collector current and accelerating voltage at 130 A discharge current. The current measured by the collector in the geometric focus area grows from 0.55 to 1.1 A with the accelerating voltage increasing from 5 to 35 kV. In Fig. 2*b*, the discharge current of 170 A increases the collector current at the accelerating voltage of 5 kV to 1.5 A. Such an increase in the measured current, disproportional to the discharge current, is caused by the vacuum-arc plasma generator of the ion-plasma source “Raduga-5”. The increase in the discharge current is accompanied by the growth in the longitudinal magnetic field, ensuring the higher magnetization of plasma electrons and, as a consequence, the growth in the transportation efficiency of the plasma flow. When the accelerating voltage reaches 35 kV, the measured current increases to 3.1 A.

The higher accelerating voltage improves the ion energy. With regard to the average charge of chromium ions at 35 kV accelerating voltage, the ion energy reaches 70 keV, i.e., the beam ion energy increases by approximately 2000 times compared to the plasma ion energy. Based on the law of the current continuity, this increase in the ion speed reduces the ion beam density by more than 40 times, which should improve conditions for the space charge compensation of the beam ions, provided that parameters of the plasma previously injected into the drift space are preserved.

Research in this field shows, however, that the current growth is not associated with the dynamics of changes in the ion current density depending on the accelerating voltage. Moreover, oscilloscope patterns of the power density of the repetitively-pulsed ion beam significantly differ from thermocouple and pyrometer recordings. It is thus assumed that the ion-induced electron emission has a significant effect on the current measured.

In this respect, we study the ion-induced electron emission and its influence on both the current and density measurements and the formation, focusing, and transportation of the high-power density ion beam. The experimental parameters include 450 μs pulse duration, 0.1 to 40 kV accelerating voltage, 2 pps pulse frequency (to avoid the collector overheat at accelerating voltage over 5 kV). The current is measured by the collector with a diameter 277 mm to study the influence of the accelerating voltage on the ion-induced electron emission. The anode diameter of the arc

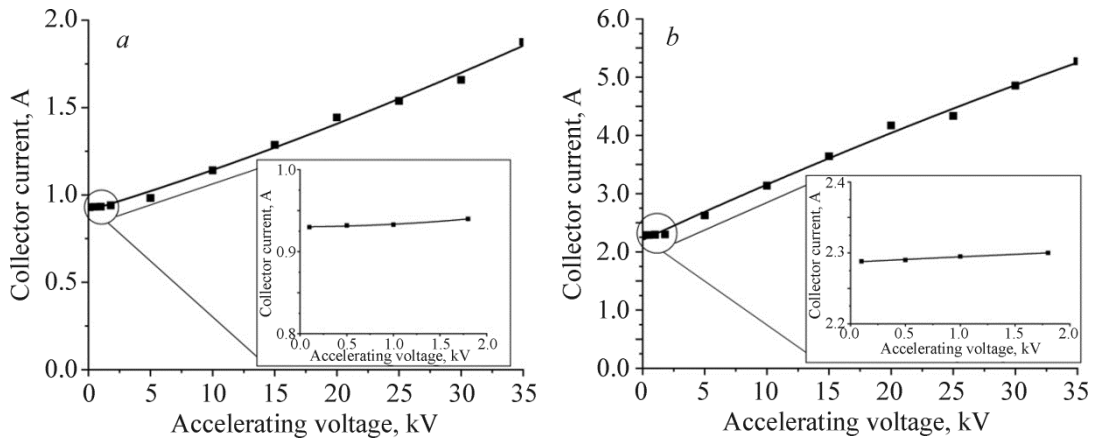


Fig. 3. Dependences between total current on solid collector and accelerating voltage at different discharge currents: *a* – 130 A, *b* – 170 A.

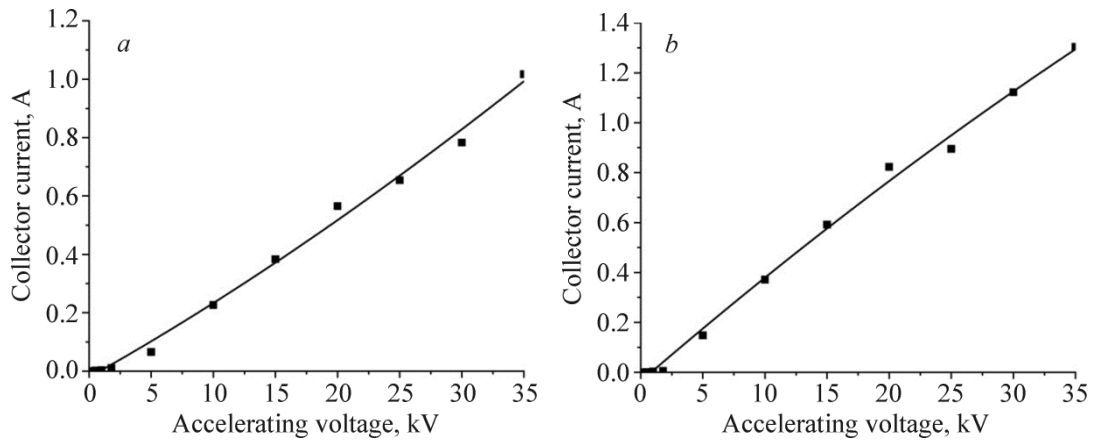


Fig. 4. Dependences between ion-electron emission of chromium ion beam at different discharge currents: *a* – 130 A, *b* – 170 A.

evaporator is 178 mm. The collector completely locks the plasma flow from the arc evaporator. The dependence between the current and accelerating voltage ranging between 0.1 and 1.8 kV, is studied to measure the ion current saturation from the plasma. As can be seen from Fig. 3*b*, the current slightly changes with increasing accelerating voltage. This current is determined by the ion current saturation from the vacuum-arc discharge plasma, which is 0.9 A at 130 A discharge current. When the discharge current is 170 A, the current measured at 0.1 to 1.8 kV accelerating voltage, reaches 2.4 A, as presented in Fig. 4.

The higher accelerating voltage of 35 kV increases the measured current to 1.83 A at 130 A and to 5.24 A at 170 A. Assuming that the measured current growth depends on the accelerating voltage and, accordingly, the ion energy is determined by the ion-induced electron emission, the dependences in Fig. 3 allow to determine the ion-induced electron emission, depending on the accelerating voltage. Figure 4 illustrates the dependences of the ion-induced electron emission for the chromium ion beam generated at 130 and 170 A discharge currents.

One can see that changes in the discharge current do not significantly affect the ion-induced electron emission. The maximum value of the ion-induced electron emission is 1.3 at the average energy of chromium ions of ~ 70 keV. The comparative analysis of dependences in Figs. 2 and 3 allows us to conclude that the current density growth by several orders of magnitude due to the ballistic beam focusing does not noticeably affect the ion-induced electron

emission. According to Fig. 2, the increase in the accelerating voltage from 5 to 35 kV, provides a two-fold increase in the measured current, that matches the data presented in Fig. 3.

A difficult measurement accuracy of the ion beam current is determined by the ion-induced electron emission, which is important to the space charge neutralization. According to [2, 3], at 2 kV accelerating voltage, the plasma electron emission in the accelerating gap through the grid cells, provides the formation of the virtual anode and disrupts the transportation of ballistic beam focusing on the target. At low ion energies, ion-induced electron emission from the target does not compensate the loss of plasma electrons. In these experiments, in the chromium ion beam generation, the ion energy varies from 10 to 70 keV with respect to the average charge composition of the plasma. A multiple growth in the ion energy increases the ion-induced electron emission and thus solves the problem of a stable transportation of the ballistic beam focusing at long pulses. The detection of the ion-induced induced electron emission is also important for the correct assessment of the power density, since the collector current is a sum of the ion current and ion-induced electron emission. Using the multi-collector system, we show that the maximum current density is achieved on a 2 cm distance from geometric focusing. At 170 A discharge current, the maximum current density, averaged over 16 pulses, reaches 2.8 A/cm^2 . The maximum power density in the ion beam approaches to 100 kW/cm^2 at 35 kV accelerating voltage. It should be noted that the unstable nature of the ion emission can increase the power density in individual pulses by more than 2 times.

CONCLUSIONS

This work studied the formation of high-intensity submillisecond chromium ion beams with the high pulse power density. It was shown that the ion-induced electron emission in the energy range from fractions to 70 keV affected the space charge neutralization and the measurement accuracy of the ion beam parameters. It was found that at high ion energies, the virtual anode effect did not appear, and the formation of ion beams with a high pulse duration occurred. The maximum current density averaged over 16 pulses, was 2.8 A/cm^2 at 170 A discharge current. The maximum power density was close to 100 kW/cm^2 at 35 kV accelerating voltage. The unstable nature of the ion emission from the vacuum arc plasma increased the power density in individual pulses by more than 2 times.

COMPLIANCE WITH ETHICAL STANDARDS

Conflicts of interest

The authors declare no conflict of interest.

Funding

This work was financially supported by the Russian Science Foundation (Project No. 22-1900051). <https://rscf.ru/project/22-19-00051/>.

Financial interests

The authors declare they have no financial interests.

Non-financial interests

None.

REFERENCES

1. M. I. Current, *Industrial Accelerators and Their Applications*, World Scientific (2012), pp. 9–56; DOI: 10.1142/9789814307055_0002.
2. F. F. Komarov and V. N. Yuvchenko, *Tech. Phys.*, **48**, No. 6, 717–721 (2003); <https://doi.org/10.1134/1.1583824>.
3. L. J. Pranjavicius and Y. J. Dudonis, *Modification of Properties of Solids with Ion Beams* [in Russian], Mokslas, Vilnius (1980).
4. I. A. Abroyan, A. N. Andronov, and A. I. Titov, *Basic Physics of Electronic and Ion Technology* [in Russian], Vysshaya shkola, Moscow (1984).
5. F. F. Komarov, *Ion Implantation in Metals* [in Russian], Metallurgiya, Moscow (1990).
6. M. I. Guseva, *Phys. Chem. Mech. Surf.*, **4**, 27–50 (1982).
7. J. K. Hirvonen and C. M. Preece, *Ion Implantation Metallurgy*, Academic Press, New York (1980).
8. H. Ryssel and I. Ruge, *Ion Implantation*, John Wiley & Sons, New York (1986).
9. J. M. Poate, G. Foti, and D. C. Jacobson, *Surface Modification and Alloying by Laser Ion, and Electron Beams*, Springer US, New York (2013).
10. J. S. Williams and J. M. Poate, *Ion Implantation and Beam Processing*, Academic Press, New York (1984).
11. R. Wei, *Surf. Coat. Tech.*, **83**, No. 1-3, 218–227 (1996); [https://doi.org/10.1016/0257-8972\(95\)02828-5](https://doi.org/10.1016/0257-8972(95)02828-5).
12. P. J. Wilbur, *et. al.*, *Surf. Coat. Tech.*, **83**, No. 1-3, 250–256 (1996); [https://doi.org/10.1016/0257-8972\(95\)02830-7](https://doi.org/10.1016/0257-8972(95)02830-7).
13. A. I. Ryabchikov, *et. al.*, *Vacuum*, **143**, 447–453 (2017); <https://doi.org/10.1016/j.vacuum.2017.03.011>.
14. A. I. Ryabchikov, *et. al.*, *Metals*, **13**, No. 9, 1604 (2023); <https://doi.org/10.3390/met13091604>.
15. A. I. Ryabchikov, *IEEE Trans. Plasma Sci.*, **49**, No. 9, 2529–2534 (2021); DOI: 10.1109/TPS.2021.3073942.
16. A. I. Ryabchikov, D. O. Vakhrushev, and S. V. Dektyarev, *Nucl. Instrum. Methods. Phys. Res.*, No. 1057, 168711 (2023); <https://doi.org/10.1016/j.nima.2023.168711>.